Performance Improvement for Computer-Generated Holographic Stereogram Based on Integral Imaging

Zi Wang[1], Guoqiang Lv[1,2], and Qibin Feng[1]

[1]National Engineering Laboratory of Special Display Technology, National Key Laboratory of Advanced Display Technology, Academy of Photoelectric Technology, Hefei University of Technology, Hefei, Anhui 230009, China
[2]School of Instrumentation and Opto-Electronics Engineering, Hefei University of Technology, Hefei, Anhui 230009,China
Keywords:Computer holography; integral imaging; holographic stereogram.

ABSTRACT

We want to introduce several recent works for improving the performance of integral imaging (II) based holographic stereogram (HS). First, we have proposed a resolution-enhanced II-based HS using the moving array lenslet technique (MALT). [1] Second, we have proposed the concept of resolution priority HS (RPHS) for the first time, which is based on the principle of resolution priority II, by adding a quadratic phase term on the conventional Fourier transform. [2] Finally, a simple and fast algorithm for computer-generated hologram (CGH) based on pinhole-type II using a look-up table was proposed. [3]

1 INTRODUCTION

Holography is considered as the final form of the three-dimensional (3D) display technique since it truly reconstructs the wavefront of the 3D scene. However, the conventional holographic recording uses a laser interference optical system, which can only be operated in a laboratory. With the development of computer technology, the computer-generated hologram (CGH) can be used to reconstruct 3D images without optical holographic recording. The CGH is often generated by simulating the wave propagation from object points or slices to the hologram plane[4]. However, because the optical transmission processes of each point or slice are independent, the occlusion and shading information of the 3D scene are hard to present.

Holographic stereogram (HS) is an effective way to address these issues by using multi-view images[5]. It is divided into many hogels (hologram element), and each hogel emits a set of plane waves to reproduce the light field. However, capturing abundant multi-view images of real objects is one difficulty of HS. The lens array can be used to capture multi-view images efficiently, which is also a fundamental part of II[6]. Thus, there have been many researches reported on the generation of holograms based on II, such as the diffraction calculation method[7], the orthographic projection image method[8], the ray sampling method[9]. Ichihashi et al. proposed a real-time II-based HS display system which used a lens array to capture EIA and each element image (EI) is converted into a corresponding hogel by fast Fourier transform (FFT)[10]. Since the holographic data was transformed from II data, this technique inherited the drawbacks of II, such as the low sampling rate and the low quality reconstructed images.

Several recent works for improving the performance of integral imaging based HS are introduced in this paper. In section 2, we will introduce the conventional II based HS. In section 3, we will introduce the proposed resolution-enhanced II-based HS using MALT. In section 4, the concept of resolution priority HS will be introduced. And in section 5, the proposed algorithm for computer-generated hologram (CGH) based on pinhole-type II using a look-up table will be introduced.

2 Conventional II based HS

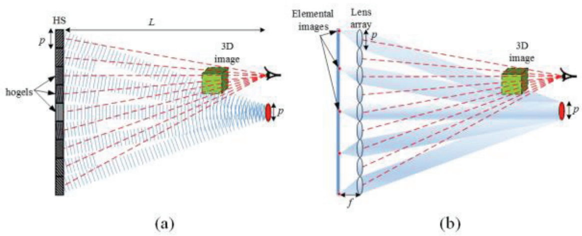

Fig. 1 (a) Wavefront reconstruction principle of the holographic stereogram. (b) Wavefront reconstruction principle of DPII.

Figure 1(a) shows the wavefront reconstruction of one point in HS. Different from Fresnel hologram which reconstructs image point with spherical waves, the HS reconstructs image point using multiple plane waves with discrete directions. Figure 1(b) shows the principle of depth priority II (DPII), which is very similar to the HS. The elemental image array (EIA) (each elemental image is a parallax image of the 3D object) is placed at the front focal plane of the lens array, so the elemental lens collimates the light rays of different pixels to different directions, and voxels are formed through intersections of multiple parallel light rays. Since the display principles of HS and DPII are almost the same, Ichihashi et al. proposed to convert elemental images into hogels by FFT calculation for real-time display [10], as shown in Fig. 2.

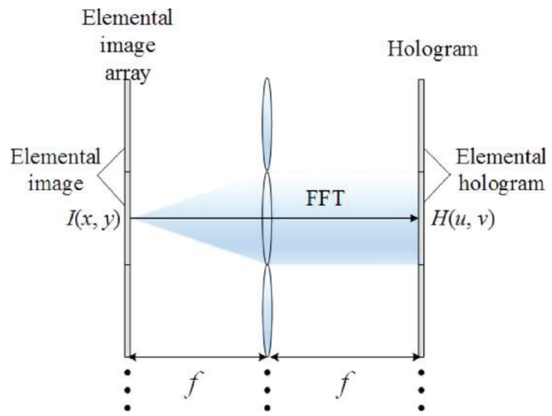

Fig. 2 Principle of the integral imaging based holographic stereogram.

Figure 2 shows the conversion process from II to HS[10]. The EIA and HS are placed at the front focal plane and the back focal plane of the lens array, respectively. According to the common knowledge in Fourier optics, an exact Fourier transform of an object can be obtained at the back focal plane of a lens if it is placed at the front focal plane of the lens. Thus, to each elemental lens, the elemental hologram $H(u,v)$ behind it is the exact Fourier transform of the elemental image $I(x,y)$ in front of it. We can obtain the following Fourier transform relation:

$$H(u,v)=\frac{1}{j\lambda f}\iint_{-\infty}^{\infty} I(x,y)\exp[-j\frac{2\pi}{\lambda f}(xu+yv)]dxdy$$

where λ is the wavelength and *f* is the focal length of the lens array. However, since it is an II-based HS, the low sampling rate of II is inherited through the conversion process and will lead to a low image quality.

3 Resolution-enhanced II-based HS using MALT

To increase the sampling rate in II-based HS, the MALT was adopted in the proposed method as shown in Fig. 3. Before the data conversion, multiple EIAs captured by MALT are prepared. At the virtual conversion process, each sequential EIA is transformed to the corresponding HS sequence through FFT calculations of elemental images. All the HS sequences are shifted and added together to synthesize the final hologram.

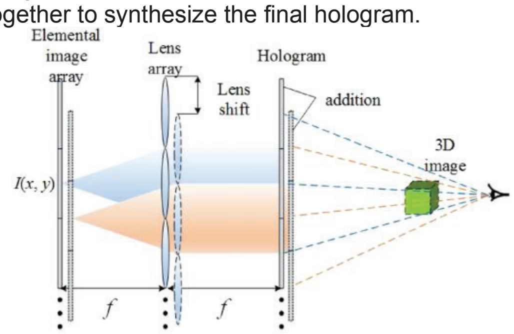

Fig. 3 Principle of proposed resolution-enhanced II-based HS using MALT.

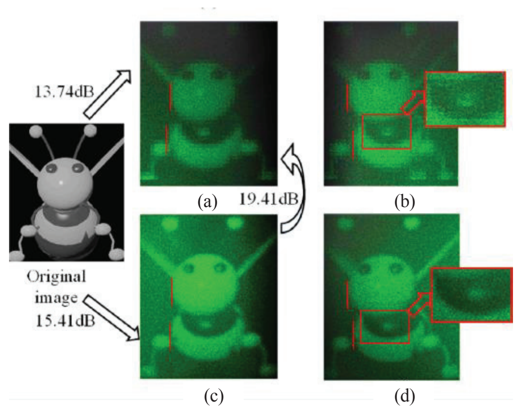

Fig. 4 . Reconstructed results.

Figures 4(a) and 4(b) show the optically reconstructed images of the bee model without MALT captured from different directions. Figures 4(c) and 4(d) show the optically reconstructed images of the bee model with MALT captured from different directions. The PSNR for Figs. 4(a) and 4(c) are 13.74 dB and 15.41 dB, respectively, so an improvement of 1.67 dB is obtained.

4 Resolution priority HS

Different from DPII which performs better at depth range, RPII has higher lateral resolution[11]. Figure 5(a) shows the principle of RPII. The gap between EIA and lens array is slightly different from (larger or smaller than) the focal length, so there exist a privileged plane in the reconstruction space, the so-called IRP, which is conjugate with the EIA plane. In such plane the object point is reconstructed with very good quality (see point A), which is very similar to the reconstruction of Fresnel hologram. Each lens emits spherical waves which are focused on the IRP. As the object point goes far away from the IRP, the reconstructed quality degrades. Thus, the depth range of RPII is limited, and the 3D image must be located around the IRP. The IRP is also called as the central depth plane (CDP). Nevertheless, the resolution of reconstructed images in the RPII is still better than in the DPII over a long depth range.

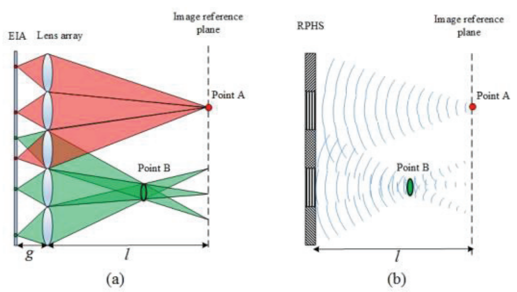

Fig. 5 (a) Wavefront reconstruction and display principle of RPII. (b) Wavefront reconstruction and display principle of proposed RPHS.

Based on the RPII, we proposed the RPHS to realize high lateral resolution as shown in Fig. 5(b). Different from conventional HS which emits plane waves, the RPHS emits spherical waves which are focused on the IRP. The object points at the IRP are reconstructed perfectly and objects points around the IRP are reconstructed with good quality. Just as the RPII has higher resolution than DPII, the proposed RPHS also has higher resolution than conventional HS. To obtain such RPHS, a modified version of Fig. 2 is adopted in Fig. 6. The EIA is placed in front of the lens array by a distance of g, and the hologram is placed at the back focal plane. According to Fourier optics , if an object I(x, y) is placed in front of the lens by a distance of g, we can obtain the light distribution H(u, v) at the back focal plane as:

$$H(u,v)=\frac{A\exp[\frac{j\pi}{\lambda f}(1-\frac{g}{f}(u^2+v^2))]}{j\lambda f}\iint_{-\infty}^{\infty}I(x,y)\exp[-j\frac{2\pi}{\lambda f}(xu+yv)]dxdy$$

where λ is the wavelength and f is the focal length of the lens array. Ignoring the constant value, Eq. (3) can be simplified as:

$$H(u,v)=\exp[\frac{j\pi}{\lambda f}(1-\frac{g}{f})(u^2+v^2)]\bullet FFT[I(x,y)]$$

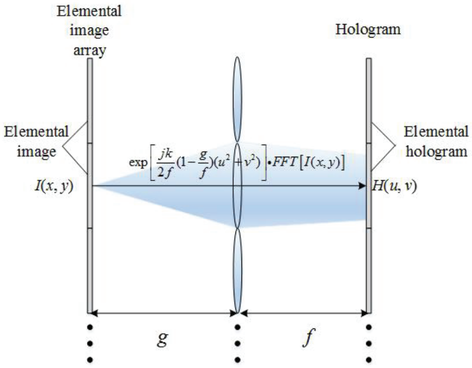

Fig. 6 Conversion process from RPII to RPHS by adding a quadratic phase term on the conventional FFT.

Figures 7(a) and 7(b) show the optical reconstruction results of conventional HS captured from different directions, and Figs. 7(c) and 7(d) show the optical reconstruction results of proposed RPHS captured from different directions. It is confirmed that the RPHS has higher resolution than conventional HS. The relative shift between different parts confirms the 3D nature of the holographic image.

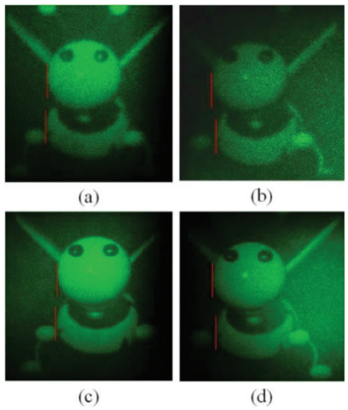

Fig. 7 (a) and (b) Optical reconstruction results of conventional HS. (c) and (d) Optical reconstruction results of proposed RPHS.

5 Computer-generated hologram (CGH) based on pinhole-type II

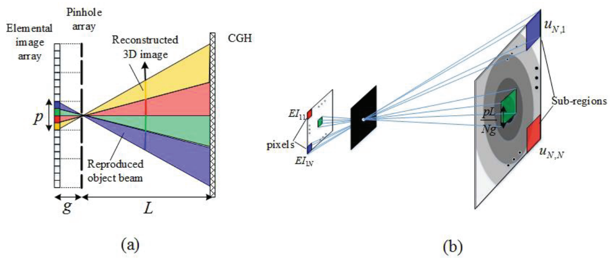

Fig. 8 (a) Principle of proposed method. (b)Light rays emitted from one pinhole.

Figure 8(a) shows the principle of proposed method. The 3D image is reconstructed by the pinhole type II system, and the CGH plane is used to record the object beam by simulating light propagation from pinholes to CGH. The light emitted from each pixel of EI can only pass through the corresponding pinhole, so each pinhole can be thought as a point light source which emits different pyramid-shaped light rays in different directions, as shown in Fig. 8(b) in which only the center pinhole is drawn. The intensities of different light rays are determined by the pixel values of EI. To the center pinhole, the recorded complex amplitude $u(x, y)$ on the CGH can be divided into many square sub-regions, and the number of sub regions is equal to that of pixels of EI. Assuming that the sub-region number or pixel number of EI in one dimension is N, the (k,l)-th sub-region $u_{kl}(x, y)$ is related to the $(N+1-k, N+1-l)$-th pixel of the center EI, and can be calculated using ray-tracing technique:

$$u_{kl}(x,y)=\frac{EI^{0,0}_{N+1-k,N+1-l}}{R}\exp(i\frac{2\pi}{\lambda}R),\quad (k-1)\frac{pL}{Ng}\le x<k\frac{pL}{Ng},(k-1)\frac{pL}{Ng}\le y<k\frac{pL}{Ng}$$

where $R=\sqrt{(x-xp)^2+(y-yp)^2+L^2}$ is the distance between the center pinhole (xp, yp) and a coordinate (x, y) on the (k,l)-th sub-region of CGH, and L is the perpendicular distance between the CGH and the pinhole array, and $EI^{0,0}_{N+1-k,N+1-l}$ is the intensity value of the $(N+1-k, N+1-l)$-th pixel of the center EI. Here, the superscript (0,0) means that the center EI is numbered as the (0,0)-th EI. And p is the pitch of pinhole or EI, and g is the distance between pinhole array and EI array. By summing all of the sub-regions, we get the complex amplitude $u(x, y)$ of the center pinhole on the CGH:

$$u(x,y)=\sum_{k}^{N}\sum_{l}^{N}u_{kl}(x,y)$$

Next, the LUT method is applied to Eq. (1). The unity amplitude diffraction pattern of the (k, l)-th sub-region $v_{kl}(x, y)$ is pre-calculated and stored as:

$$v_{kl}(x,y)=\frac{1}{R}\exp(i\frac{2\pi}{\lambda}R),\qquad (k-l)\frac{pL}{Ng}\le x<k\frac{pL}{Ng},(k-l)\frac{pL}{Ng}\le x<k\frac{pL}{Ng}$$

then the complex amplitude $u(x, y)$ of the center pinhole on the CGH is obtained as:

$$u(x,y)=\sum_{k}^{N}\sum_{l}^{N}v_{kl}(x,y)\cdot EI_{N+1-k,N+1-l}^{0,0}$$

Instead of directly computing the diffraction patterns of the center pinhole using ray-tracing method, each pixel $EI_{N+1-k,N+1-l}^{0,0}$ is just mapped into the corresponding pre-calculated sub-region $v_{kl}(x,y)$ and combined to generate the diffraction pattern. So far, the unity amplitude diffraction pattern of the center pinhole is pre-calculated as N×N sub-regions and is stored in a LUT. And the diffraction patterns for other pinholes can be obtained by simply shifting and tiling the pre-calculated sub-regions.

Figure 9 shows the numerical reconstruction results from nine different viewing directions, which can be generated from different parts of the CGH. The relative shift between different parts is clearly observed, confirming successful reconstruction of the 3D object.

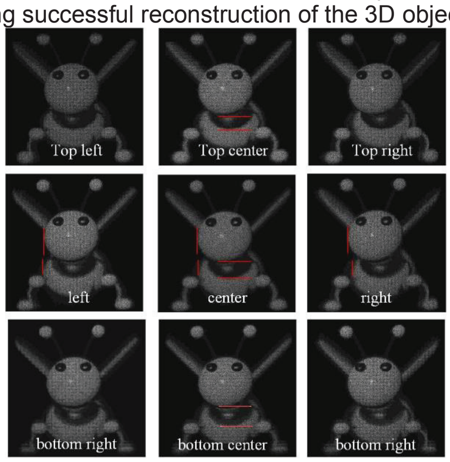

Fig. 9 Numerical reconstruction results from different viewing directions.

6 Conclusion

Several recent works for improving the performance of integral imaging (II) based holographic stereogram (HS) are introduced. First, due to the limited sampling rate, the quality of reconstructed images of conventional II-based HS is not high. To increase the sampling rate,the the moving array lenslet technique (MALT) is adopted in this paper. [1] Second, we have proposed the concept of resolution priority HS (RPHS) for the first time, which is based on the principle of resolution priority II, by adding a quadratic phase term on the conventional Fourier transform. [2] Compared to the conventional II-based HS, the proposed RPHS has higher resolution. Finally, a simple and fast algorithm for computer-generated hologram (CGH) based on pinhole-type II using a look-up table was proposed. [3]

REFERENCES

[1] Wang Z, Chen R S, Zhang X, et al. Resolution-enhanced holographic stereogram based on integral imaging using moving array lenslet technique[J]. Applied Physics Letters, 2018, 113(22): 221109.

[2] Wang Z, Lv G Q, Feng Q B, et al. Resolution priority holographic stereogram based on integral imaging with enhanced depth range[J]. Optics express, 2019, 27(3): 2689-2702.

[3] Wang Z, Lv G, Feng Q, et al. Simple and fast calculation algorithm for computer-generated hologram based on integral imaging using look-up table[J]. Optics express, 2018, 26(10): 13322-13330.

[4] P. W. M. Tsang and T. C. Poon, "Review on the state-of-the-art technologies for acquisition and display of digital holograms," IEEE Trans. Ind.Inf. 12(3), 886–901 (2016).

[5] McCrickerd J T, George N. Holographic stereogram from sequential component photographs[J]. Applied Physics Letters, 1968, 12(1): 10-12.

[6] Wang Z, Wang A, Wang S, et al. Resolution-enhanced integral imaging using two micro-lens arrays with different focal lengths for capturing and display[J]. Optics express, 2015, 23(22): 28970-28977.

[7] Mishina T, Okui M, Okano F. Calculation of holograms from elemental images captured by integral photography[J]. Applied optics, 2006, 45(17): 4026-4036.

[8] Park J H, Kim M S, Baasantseren G, et al. Fresnel and Fourier hologram generation using orthographic projection images[J]. Optics express, 2009, 17(8): 6320-6334.

[9] Wakunami K, Yamaguchi M, Javidi B. High-resolution three-dimensional holographic display using dense ray sampling from integral imaging[J]. Optics letters, 2012, 37(24): 5103-5105.

[10] Ichihashi Y, Oi R, Senoh T, et al. Real-time capture and reconstruction system with multiple GPUs for a 3D live scene by a generation from 4K IP images to 8K holograms[J]. Optics express, 2012, 20(19): 21645-21655.

[11] Navarro H, Martínez-Cuenca R, Molina-Martín A, et al. Method to remedy image degradations due to facet braiding in 3D integral-imaging monitors[J]. Journal of Display Technology, 2010, 6(10): 404-411.